COMMUNICATION

A Highly Selective and Sensitive Chemiluminescent Probe for Real-Time Monitoring of Hydrogen Peroxide in Cells and Animals

Sen Ye,[a]+ Nir Hananya,[b]+ Ori Green,[b] Hansen Chen,[c] Angela Qian Zhao,[a] Jiangang Shen,[c] Doron Shabat,*[b] and Dan Yang*[a]

[a] Dr. S. Ye, A. Q. Zhao, Prof. Dr. D. Yang
Morningside Laboratory for Chemical Biology and Department of Chemistry
HKU Shenzhen Institute of Research and Innovation (HKU-SIRI)
The University of Hong Kong
Pokfulam Road, Hong Kong, P. R. China
E-mail: yangdan@hku.hk
[b] Dr. N. Hananya, Dr. O. Green, and Prof. Dr. D. Shabat
School of Chemistry, Faculty of Exact Sciences
Tel Aviv University
Tel Aviv 69978 (Israel)
E-mail: chdoron@post.tau.ac.il
[c] Dr. H.-S. Chen, Prof. Dr. J.-G. Shen
School of Chinese Medicine
The University of Hong Kong
Pokfulam Road, Hong Kong, P. R. China
[+] These two authors made equal contribution to this paper.

Supporting information for this article is given via a link at the end of the document.

Abstract: Selective and sensitive molecular probes for hydrogen peroxide (H_2O_2), which plays diverse roles in oxidative stress and redox signalling, are urgently needed to investigate the physiological and pathological effects of H_2O_2. A lack of reliable tools for *in vivo* imaging has hampered the development of H_2O_2 mediated therapeutics. By combining a specific tandem Payne/Dakin reaction with a chemiluminescent scaffold, **H_2O_2-CL-510** was developed as a highly selective and sensitive probe for detection of H_2O_2 both *in vitro* and *in vivo*. A rapid 430-fold enhancement of chemiluminescence was triggered directly by H_2O_2 without any laser excitation. Arsenic trioxide induced oxidative damage in leukemia was successfully detected. In particular, cerebral ischemia-reperfusion injury induced H_2O_2 fluxes were visualized in rat brains using **H_2O_2-CL-510**, providing a new chemical tool for real-time monitoring of H_2O_2 dynamics in living animals.

As a transient reactive oxygen species (ROS), hydrogen peroxide (H_2O_2) could diffuse across the cellular membrane and play diverse roles in oxidative damaging and redox signaling.[1] Recent efforts to manually modulate H_2O_2 levels have shown great potential in developing ROS mediated therapeutics.[2] For example, vitamin C was confirmed to be a pro-oxidant which could induce H_2O_2 burst and sensitize certain cancer cells.[3] Chemodynamic therapy to kill tumor cells relies heavily on H_2O_2 overproduction in tumor microenvironment,[4] while removing excessive H_2O_2 in unfavorable sites could be used to attenuate inflammatory and apoptotic activities during ischemia-reperfusion treatment.[5] Selective and sensitive monitoring of H_2O_2 levels is thus critical for developing new therapeutics based on H_2O_2 modulation.

There has been a constant interest in developing selective and sensitive H_2O_2 sensing strategies, including boronic acid deprotection,[6] Baeyer-Villiger reaction,[7] tandem Payne/Dakin reaction,[8] and fluorescent protein sensors,[9] etc. Those H_2O_2 probes have been widely applied in live cell imaging to elucidate the important roles of cellular H_2O_2 in oxidative stress and signaling.[6–9] Some of the probes further push the boundaries of H_2O_2 bio-imaging to tissue staining and transparent animal imaging, such as zebrafish imaging.[10] However, the majority of them are fluorescent probes, therefore laser excitation is required, and autofluorescence and photon-scattering caused by animal skin are inevitable.

To address this issue, chemiluminescent and bioluminescent probes were developed as an alternative strategy for *in vivo* H_2O_2 imaging. As shown in Scheme 1, previous strategies are either based on dye/peroxalate system[11] or luciferin/luciferase system.[12] Both strategies successfully detected endogenous H_2O_2 burst in living mice, however, the dye/peroxalate system usually requires complicated nanoparticle fabrication, and the luciferin/ luciferase system requires luciferase-expressing animals, plus ATP, magnesium ion, and oxygen for H_2O_2 imaging. Recently, the modified Schaap's dioxetane was discovered to be 3,000-time brighter than previous version, and has become a research hotspot in bioimaging.[13] Bearing peroxide bond and fluorophore in one scaffold, this phenoxy-dioxetane derivative could emit light directly, thus was explored to develop reaction-based probes for metabolite sensing.[14] As a continuous effort to develop molecular probes for advancing redox biology, herein we report the design, synthesis and application of **H_2O_2-CL-510**, a small-molecule chemiluminescent probe that can be triggered by H_2O_2 to give strong emission without any excitation. Built on a

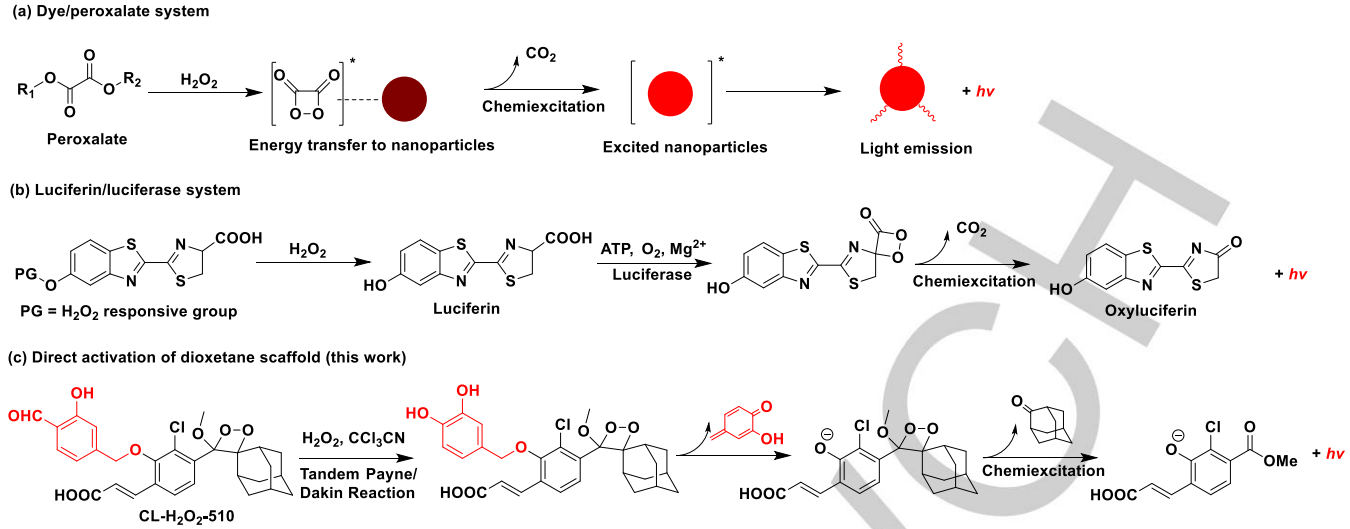

Scheme 1. General strategies for chemiluminescent and bioluminescent H_2O_2 sensing. (A) Dye/peroxalate system. (B) Luciferin/luciferase system. (C) Direct activation of phenoxy-dioxetane by tandem Payne/Dakin reaction.

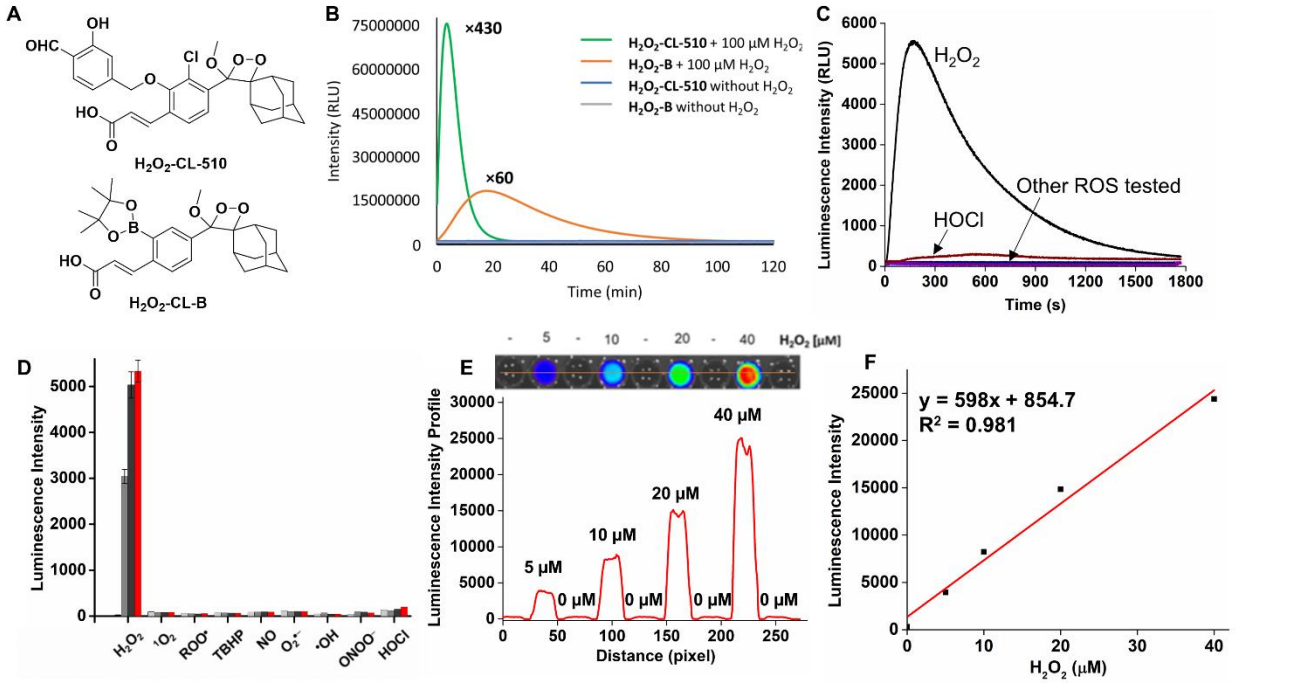

Figure 1. (A) Chemical structures of H_2O_2 probes **H_2O_2-CL-510** and **H_2O_2-CL-B**. (B) Chemiluminescence kinetic profile of **H_2O_2-CL-510** (10 μM, supplemented with 100 μM CCl_3CN) and **H_2O_2-CL-B** (10 μM) in the presence or absence of 100 μM H_2O_2. Measurements were conducted at potassium phosphate buffer, pH 7.4, 37°C. (C) Time course of **H_2O_2-CL-510** (10 μM) reacted with various ROS (100 μM). (D) Luminescence response of **H_2O_2-CL-510** (10 μM) reacted with various ROS (100 μM), bars represent emission intensities at 0 (light grey), 1 (grey), 2 (dark grey), and 3 (red) min. (E) Luminescent image and profile of **H_2O_2-CL-510** (10 μM) treated with increasing amounts of H_2O_2 (0–40 μM). The image was acquired at 2–3 min after H_2O_2 addition. (F) Luminescence intensity of **H_2O_2-CL-510** as a function of **H_2O_2** concentrations (0–40 μM).

specific H_2O_2-mediated Payne/Dakin reaction (Scheme 1c), this novel chemiluminescent probe is very selective and sensitive towards H_2O_2, and has been successfully applied to detect H_2O_2 both *in vitro* and *in vivo*. Endogenous H_2O_2 burst in arsenic trioxide (As_2O_3) treated leukemia has been robustly detected. More importantly, for the first time, cerebral ischemia-reperfusion injury induced H_2O_2 fluxes in brain of living rats have been visualized with **H_2O_2-CL-510**. The overall high selectivity and sensitivity, rapid response, and excellent signal-to-noise ratio for *in vivo* imaging make it an ideal tool for real-time monitoring of H_2O_2 dynamics.

Our design is based on a masked phenoxy-dioxetane platform that could be selectively deprotected by H_2O_2. Upon reaction with H_2O_2, the salicylaldehyde (sensing moiety) is oxidized to a catechol, followed by a subsequent ether cleavage to unmask the phenoxy-dioxetane, which further undergoes chemiexcitation to release the chemiluminescence (Scheme 1c). The designed probe **H_2O_2-CL-510** was successfully synthesized and characterized (see supporting information).

With **H_2O_2-CL-510** in hand, we first evaluated its chemiluminescent response towards H_2O_2 in potassium phosphate buffer. As shown in Figure 1, upon treatment with 100 μM H_2O_2, **H_2O_2-CL-510** (10 μM) produced a 430-fold

enhancement of chemiluminescence signal within 3 min (Figures 1B, S1 and S2), which makes **H_2O_2-CL-510** a fast responding molecular probe for H_2O_2 detection. This fast turn-on also confirms that the ether linker could be efficiently cleaved similarly to the carbamate linker in our previous design.[8] In comparison, under the same conditions, the previously reported **H_2O_2-CL-B** responded to H_2O_2 much slower,[13c,13f] with maximal luminescence enhancement of 60-fold after 17 min. More importantly, **H_2O_2-CL-510** is extremely selective towards H_2O_2, as other potential competing ROS only triggered negligible responses (Figures 1C and 1D). To test its sensitivity towards physiological concentrations of H_2O_2 in IVIS Spectrum imaging system, 10 μM **H_2O_2-CL-510** was treated with 0–40 μM of H_2O_2 in a 96-well plate. Due to the superior sensitivity of our sensing and imaging strategy, low levels of H_2O_2 were successfully visualized with high signal-to-noise ratio and in a dose-dependent manner, whereas auto-luminescence signal of **H_2O_2-CL-510** without H_2O_2 treatment was negligible (Figures 1E and S3). In particular, a linear relationship of luminescence intensities and H_2O_2 concentrations was observed in Figure 1F, the detection limit was determined to be less than 5 μM, and an estimation based on the linear calibration (3σ/k) suggests that as low as 7.1 nM may be detectable.

The rapid chemiluminescent response, high signal-to-noise ratio, excellent selectivity, low toxicity (Figure S4) and superiority to existing probes suggest that **H_2O_2-CL-510** could be used as a powerful molecular probe to study H_2O_2 related biological processes. Arsenic trioxide has been found to be a very effective drug to treat acute promyelocytic leukemia possibly by inducing ROS.[15,16] We would like to address this issue with our selective probe **H_2O_2-CL-510**.

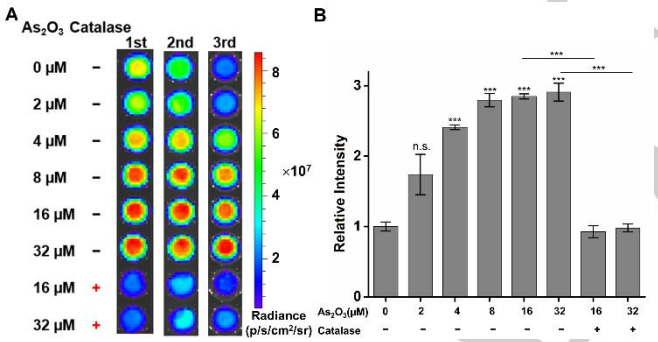

Figure 2. Chemiluminescent imaging of THP-1 cells. Cells were treated with increasing amounts of As_2O_3, then **H_2O_2-CL-510** (10 μM, 0.1% DMF, 100 μM CCl_3CN) was added, and chemiluminescence images were acquired. PEG-catalase was added in intervention groups. (A) Representative cell images with or without As_2O_3 treatment. (B) Quantifications of chemiluminescence signals from the cells. Data are mean ± s.e.m., *n* =3. Statistical analyses were performed with a Student's *t* test where n.s.: not significant, ***: $p < 0.001$.

In this investigation, THP-1 cells, a human monocytic leukemia cell line, were first treated with increasing amounts of As_2O_3 (0–32 μM) for 24 h. Prior to imaging, cell-permeable catalase-polyethylene glycol (PEG-catalase) was added into intervention groups to remove H_2O_2. Then **H_2O_2-CL-510** (10 μM) was added, and chemiluminescent images were acquired. As shown in Figure 2A, As_2O_3 challenged H_2O_2 fluxes could be robustly visualized in a chemiluminescent mode with **H_2O_2-CL-510**. While 4 μM As_2O_3 already induced a significant level of cellular H_2O_2, the luminescence intensity seemed to reach its maximum with 8 μM As_2O_3 treatment, and higher As_2O_3 dosages did not further increase H_2O_2 levels (Figure 2B). More importantly, the chemiluminescent signal could be efficiently attenuated by PEG-catalase, which confirms that our new probe could detect cellular H_2O_2 fluxes in a selective manner. The application of **H_2O_2-CL-510** in 96-well plate imaging also provides a starting point for high-throughput screening for other therapeutic reagents to treat leukemia.

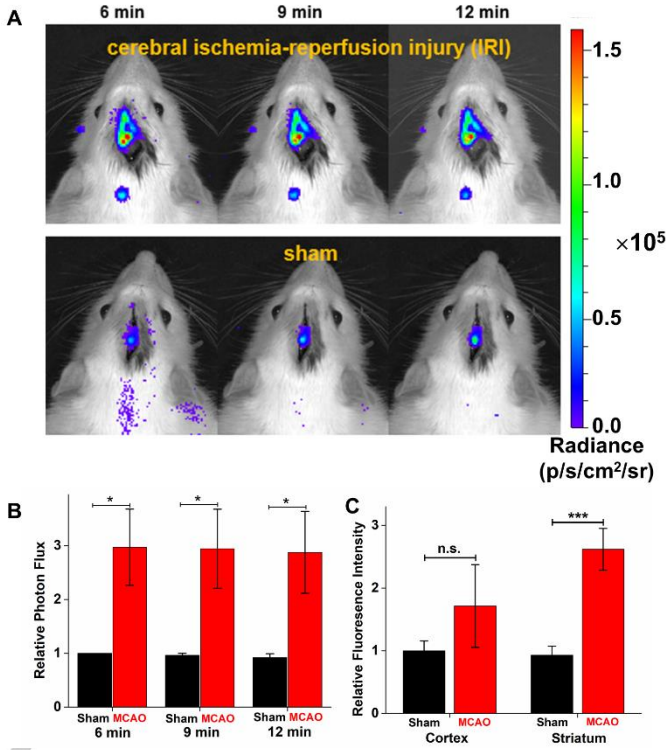

Figure 3. *In vivo* chemiluminescent imaging of **H_2O_2-CL-510** in response to H_2O_2 production in rat brain during ischemia-reperfusion injury. **H_2O_2-CL-510** (1 μL 10 mM in DMF mixed with 4 μL 10 mM CCl_3CN in water) was intraventricularly injected into rat brain before imaging. (A) Representative images of rat in MCAO group and sham group. (B) Quantifications of photon fluxes released by **H_2O_2-CL-510** in rat brain. (C) Quantifications of fluorescence intensities in cortex or striatum of brain tissue stained by H_2O_2 fluorescence probe **HKPerox-4** (10 μM). Data are mean ± s.e.m., *n* =3. Statistical analyses were performed with a Student's *t* test where n.s.: not significant, *: $p < 0.05$, ***: $p < 0.001$.

After confirming that H_2O_2-mediated Payne/Dakin reaction of **H_2O_2-CL-510** performs very well in buffer and *in vitro*, we applied the probe to *in vivo* real-time imaging. In this study, we investigated the H_2O_2 dynamics induced by cerebral ischemia-reperfusion. Previous studies showed that the restoration of blood supply to treat acute stroke could produce multiple pathological damages, including leukocyte infiltration, platelet activation, and breakdown of the blood-brain barrier.[17] H_2O_2 burst might be partially responsible for those damages by inducing oxidative stress and programmed cell death.[18] However, it is very difficult for real-time monitoring of H_2O_2 in living animals under reperfusion process.[19] Our chemiluminescent probe that enables direct real-time visualization of H_2O_2 in rat brain could greatly help to investigate the complex interplays of H_2O_2 fluxes and inflammatory cascades during reperfusion injury.

In this regard, middle cerebral artery occlusion (MCAO) method was used to induce cerebral ischemia-reperfusion injury in living rats. The rats were allowed to ischemia for 2 h followed by 1 h reperfusion, and then **H_2O_2-CL-510** was injected into the ventricle of rat brain. Due to the rapid response of our probe, H_2O_2 burst after ischemia-reperfusion injury could be detected in real-time. The bright chemiluminescent signal and fast photon acquisition also enabled a time-lapse *in vivo* imaging at 6, 9, 12 min with an acquisition time of 2 min. As shown in Figures 3 and S5, cerebral ischemia-reperfusion injury could efficiently induce H_2O_2 burst in rat brain, which was visualized with **H_2O_2-CL-510**. Moreover, minimal autofluorescence and laser reflection in chemiluminescent mode ensure excellent signal-to-noise ratio for *in vivo* imaging. Further quantifications based on imaging indicate a 3-fold enhancement of photon fluxes in MCAO group compared to sham group. To examine the H_2O_2 rich brain region in MCAO rat, we further stained brain tissue with fluorescent probe **HKPerox-4** to confirm that H_2O_2 flux was primarily detected in the striatum region, while no significant increase was observed in the cortex region (Figures 3C and S6).[20] These data reveal that cerebral ischemia-reperfusion injury could rapidly induce H_2O_2 burst in rat brain, and the higher H_2O_2 levels in striatum might initiate subsequent oxidative damages and signaling processes.

In conclusion, by combining a general tandem Payne/Dakin reaction and a unique phenoxy-dioxetane chemiluminescent platform, we have designed and synthesized a novel probe **H_2O_2-CL-510** for H_2O_2 detection. The rapid H_2O_2 sensing and unique chemiexcitation emission ensure the high selectivity and sensitivity of **H_2O_2-CL-510**, which are critical to discerning subtle signals of H_2O_2 in biological environments from those noises of competing species and autofluorescence. Although the electron deficient nitrile CCl_3CN that activates H_2O_2 for detection might have potential interference to biological systems, the low application dose and very short incubation time could keep the interference to a minimum (in fact our previous data confirmed that CCl_3CN up to 200 μM showed negligible or no cytotoxicity with 24 h incubation).[8] The successful applications of **H_2O_2-CL-510** in chemiluminescent imaging of living cells and real-time monitoring of rat brain make it a valuable imaging tool for redox biology and medicine. We anticipate that **H_2O_2-CL-510** could inspire more investigations in H_2O_2 related diagnostics and therapeutics, as well as the development of other ROS specific chemiluminescent probes for *in vivo* study.

Acknowledgements

We thank the HKU Li Ka Shing Faculty of Medicine Faculty Core Facility for support in animal imaging. This work was supported by The University of Hong Kong, Morningside Foundation, Hong Kong Research Grants Council Area of Excellence Scheme (AoE/P-705/16 to D.Y.) and National Natural Science Foundation of China (21961142011 to D.Y.). D.S. thanks the ISF-China joint funding program.

Keywords: bioimaging • chemiluminescence • hydrogen peroxide • ischemia-reperfusion • probe

[1] a) H. Sies, *Redox Biol.* **2017**, *11*, 613-619; b) B. C. Dickinson, C. J. Chang, *Nat. Chem. Biol.* **2011**, *7*, 504-511; c) C. C. Winterbourn, *Nat. Chem. Biol.* **2008**, *4*, 278-286; d) E. A. Veal, A. M. Day, B. A. Morgan, *Mol. Cell* **2007**, *26*, 1-14.

[2] a) E. Singer, J. Judkins, N. Salomonis, L. Matlaf, P. Soteropoulos, S. McAllister, L. Soroceanu, *Cell Death Dis.* **2015**, *6*, e1601; b) D. Trachootham, J. Alexandre, P. Huang, *Nat. Rev. Drug Discov.* **2009**, *8*, 579-591.

[3] J. D. Schoenfeld, Z. A. Sibenaller, K. A. Mapuskar, B. A. Wagner, K. L. Cramer-Morales, M. Furqan, S. Sandhu, T. L. Carlisle, M. C. Smith, T. Abu Hejleh, D. J. Berg, J. Zhang, J. Keech, K. R. Parekh, S. Bhatia, V. Monga, K. L. Bodeker, L. Ahmann, S. Vollstedt, H. Brown, E. P. Shanahan Kauffman, M. E. Schall, R. J. Hohl, G. H. Clamon, J. D. Greenlee, M. A. Howard, M. K. Schultz, B. J. Smith, D. P. Riley, F. E. Domann, J. J. Cullen, G. R. Buettner, J. M. Buatti, D. R. Spitz, B. G. Allen, *Cancer Cell* **2017**, *31*, 487-500.

[4] a) Z. Tang, Y. Liu, M. He, W. Bu, *Angew. Chem. Int. Ed.* **2019**, *58*, 946-956; *Angew. Chem.* **2019**, *131*, 958-968; b) L.-S. Lin, T. Huang, J. Song, X.-Y. Ou, Z. Wang, H. Deng, R. Tian, Y. Liu, J.-F. Wang, Y. Liu, G. Yu, Z. Zhou, S. Wang, G. Niu, H.-H. Yang, X. Chen, *J. Am. Chem. Soc.* **2019**, *141*, 9937-9945.

[5] a) D. Lee, S. Park, S. Bae, D. Jeong, M. Park, C. Kang, W. Yoo, M. A. Samad, Q. Ke, G. Khang, P. M. Kang, *Sci. Rep.* **2015**, *5*, 16592; b) S. Bae, M. Park, C. Kang, S. Dilmen, T. H. Kang, D. G. Kang, Q. Ke, S. U. Lee, D. Lee, P. M. Kang, *J. Am. Heart Assoc.* **2016**, *5*, e003697.

[6] a) E. W. Miller, A. E. Albers, A. Pralle, E. Y. Isacoff, C. J. Chang, *J. Am. Chem. Soc.* **2005**, *127*, 16652-16659; b) B. C. Dickinson, C. J. Chang, *J. Am. Chem. Soc.* **2008**, *130*, 9638-9639; c) A. R. Lippert, G. C. V. De Bittner, C. J. Chang, *Accounts Chem. Res.* **2011**, *44*, 793-804; d) L. Yuan, W. Lin, Y. Xie, B. Chen, S. Zhu, *J. Am. Chem. Soc.* **2012**, *134*, 1305-1315.

[7] a) M. Abo, Y. Urano, K. Hanaoka, T. Terai, T. Komatsu, T. Nagano, *J. Am. Chem. Soc.* **2011**, *133*, 10629-10637; b) X. Xie, X. e. Yang, T. Wu, Y. Li, M. Li, Q. Tan, X. Wang, B. Tang, *Anal. Chem.* **2016**, *88*, 8019-8025.

[8] S. Ye, J. J. Hu, D. Yang, *Angew. Chem. Int. Ed.* **2018**, *57*, 10173-10177; *Angew. Chem.* **2018**, *130*, 10330-10334.

[9] a) A. Tsourkas, G. Newton, J. M. Perez, J. P. Basilion, R. Weissleder, *Anal. Chem.* **2005**, *77*, 2862-2867; b) B. Simen Zhao, Y. Liang, Y. Song, C. Zheng, Z. Hao, P. R. Chen, *J. Am. Chem. Soc.* **2010**, *132*, 17065-17067; c) D. S. Bilan, L. Pase, L. Joosen, A. Y. Gorokhovatsky, Y. G. Ermakova, T. W. J. Gadella, C. Grabher, C. Schultz, S. Lukyanov, V. V. Belousov, *ACS Chem. Biol.* **2013**, *8*, 535-542; d) B. Morgan, K. Van Laer, T. N. E. Owusu, D. Ezeriņa, D. Pastor-Flores, P. S. Amponsah, A. Tursch, T. P. Dick, *Nat. Chem. Biol.* **2016**, *12*, 437-443.

[10] a) B. Dong, X. Song, X. Kong, C. Wang, Y. Tang, Y. Liu, W. Lin, *Adv. Mater.* **2016**, *28*, 8755-8759; b) C.-K. Wang, J. Cheng, X.-G. Liang, C. Tan, Q. Jiang, Y.-Z. Hu, Y.-M. Lu, K. Fukunaga, F. Han, X. Li, *Theranostics* **2017**, *7*, 3803-3813, c) H. Guo, G. Chen, M. Gao, R. Wang, Y. Liu, F. Yu, *Anal. Chem.* **2019**, *91*, 1203-1210; d) H. Wang, Z. He, Y. Yang, J. Zhang, W. Zhang, W. Zhang, P. Li, B. Tang, *Chem. Sci.* **2019**, *10*, 10876-10880; e) H. Guo, G. Chen, M. Gao, R. Wang, Y. Liu, F. Yu, *Anal. Chem.* **2019**, *91*, 1203-1210.

[11] a) D. Lee, S. Khaja, J. C. Velasquez-Castano, M. Dasari, C. Sun, J. Petros, W. R. Taylor, N. Murthy, *Nat. Mater.* **2007**, *6*, 765-769; b) C.-K. Lim, Y.-D. Lee, J. Na, J. M. Oh, S. Her, K. Kim, K. Choi, S. Kim, I. C. Kwon, *Adv. Funct. Mater.* **2010**, *20*, 2644-2648; c) A. J. Shuhendler, K. Pu, L. Cui, J. P. Uetrecht, J. Rao, *Nat. Biotech.* **2014**, *32*, 373-380; d) H. J. Kim, Y. H. Seo, S. An, A. Jo, I. C. Kwon, S. Kim, *Theranostics* **2018**, *8*, 1798-1807.

[12] a) G. C. Van de Bittner, E. A. Dubikovskaya, C. R. Bertozzi, C. J. Chang, *P. Natl. Acad. Sci.* **2010**, *107*, 21316-21321; b) W. Wu, J. Li, L. Chen, Z. Ma, W. Zhang, Z. Liu, Y. Cheng, L. Du, M. Li, *Anal. Chem.* **2014**, *86*, 9800-9806.

[13] a) A. P. Schaap, T.-S. Chen, R. S. Handley, R. DeSilva, B. P. Giri, *Tetrahedron Lett.* **1987**, *28*, 1155-1158; b) N. Hananya, A. Eldar Boock, C. R. Bauer, R. Satchi-Fainaro, D. Shabat, *J. Am. Chem. Soc.* **2016**, *138*, 13438-13446; c) O. Green, T. Eilon, N. Hananya, S. Gutkin, C. R. Bauer, D. Shabat, *ACS Cent. Sci.* **2017**, *3*, 349-358; d) N. Hananya, D. Shabat, *Angew. Chem. Int. Ed.* **2017**, *56*, 16454-16463; *Angew. Chem.* **2017**, *129*, 16674-16683; e) N. Hananya, D. Shabat, *ACS Cent. Sci.* **2019**, *5*, 949-959; f) P. Gopinath, A. Mahammed, T. Eilon-Shaffer, M.

Nawatha, S. Ohayon, D. Shabat, Z. Gross, A. Brik, *ChemBioChem* **2017**, *18*, 1683-1687.

[14] a) N. Hananya, O. Green, R. Blau, R. Satchi-Fainaro, D. Shabat, *Angew. Chem. Int. Ed.* **2017**, *56*, 11793-11796; *Angew. Chem.* **2017**, *129*, 11955-11958; b) O. Green, S. Gnaim, R. Blau, A. Eldar-Boock, R. Satchi-Fainaro, D. Shabat, *J. Am. Chem. Soc.* **2017**, *139*, 13243-13248; c) K. J. Bruemmer, O. Green, T. A. Su, D. Shabat, C. J. Chang, *Angew. Chem. Int. Ed.* **2018**, *57,* 7508-7512; *Angew. Chem.* **2018**, *130*, 7630-7634; d) J. Cao, W. An, A. G. Reeves, A. R. Lippert, *Chem. Sci.* **2018**, *9*, 2552-2558; e) W. An, L. S. Ryan, A. G. Reeves, K. J. Bruemmer, L. Mouhaffel, J. L. Gerberich, A. Winters, R. P. Mason, A. R. Lippert, *Angew. Chem. Int. Ed.* **2019**, *58*, 1361-1365; *Angew. Chem.* **2019**, *131*, 1375-1379; f) J. Huang, J. Li, Y. Lyu, Q. Miao, K. Pu, *Nat. Mater.* **2019**, *18*, 1133-1143.

[15] a) G. Q. Chen, J. Zhu, X. G. Shi, J. H. Ni, H. J. Zhong, G. Y. Si, X. L. Jin, W. Tang, X. S. Li, S. M. Xong, Z. X. Shen, G. L. Sun, J. Ma, P. Zhang, T. D. Zhang, C. Gazin, T. Naoe, S. J. Chen, Z. Y. Wang, Z. Chen, *Blood* **1996**, *88*, 1052-1061; b) G. Q. Chen, X. G. Shi, W. Tang, S. M. Xiong, J. Zhu, X. Cai, Z. G. Han, J. H. Ni, G. Y. Shi, P. M. Jia, M. M. Liu, K. L. He, C. Niu, J. Ma, P. Zhang, T. D. Zhang, P. Paul, T. Naoe, K. Kitamura, W. Miller, S. Waxman, Z. Y. Wang, H. de The, S. J. Chen, Z. Chen, *Blood* **1997**, *89*, 3345-3353.

[16] a) Y. Jing, J. Dai, R. M. E. Chalmers-Redman, W. G. Tatton, S. Waxman, *Blood* **1999**, *94*, 2102-2111; b) J. Yi, F. Gao, G. Shi, H. Li, Z. Wang, X. Shi, X. Tang, *Apoptosis* **2002**, *7*, 209-215; c) Y. Sánchez, D. Amrán, C. Fernández, E. de Blas, P. Aller, *Int. J. Cancer* **2008**, *123*, 1205-1214.

[17] J. Pan, A.-A. Konstas, B. Bateman, G. A. Ortolano, J. Pile-Spellman, *Neuroradiology* **2007**, *49*, 93-102.

[18] D. N. Granger, P. R. Kvietys, *Redox Biol.* **2015**, *6*, 524-551.

[19] a) X. Bai, K. K.-H. Ng, J. J. Hu, S. Ye, D. Yang, *Annu. Rev. Biochem.* **2019**, *88*, 605-633; b) F. Rezende, R. P. Brandes, K. Schröder, *Antioxid. Redox Sign.* **2017**, *29*, 585-602.

[20] **HKPerox-4** is a red fluorescent H_2O_2 probe described as YS-4-112 in following patent: D. Yang, S. Ye, J. J. Hu, **2018**, PCT Appl. No.: WO2018133859.

Entry for the Table of Contents

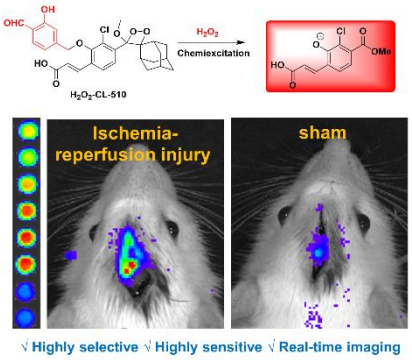

Peroxide triggered, peroxide excited. Real-time monitoring of hydrogen peroxide (H_2O_2) in rat brains has been achieved by combining a unique H_2O_2 sensing strategy and a peroxide bond excited chemiluminescent scaffold. This direct activation of phenoxy-dioxetane by tandem Payne/Dakin reaction provides a highly selective, sensitive, and rapid detection of H_2O_2 in chemical systems, cellular environment, and living animals.

Institute and/or researcher Twitter usernames: @HKUniversity, @DanYangLab

Supporting Information

69451 Weinheim, Germany

A Highly Selective and Sensitive Chemiluminescent Probe for Real-Time Monitoring of Hydrogen Peroxide in Cells and Animals

Sen Ye,[a]+ Nir Hananya,[b]+ Ori Green,[b] Hansen Chen,[c] Angela Qian Zhao,[a] Jiangang Shen,[c] Doron Shabat,*[b] and Dan Yang*[a]

[a] Dr. S. Ye, A. Q. Zhao, Prof. Dr. D. Yang
Morningside Laboratory for Chemical Biology and Department of Chemistry
HKU Shenzhen Institute of Research and Innovation (HKU-SIRI)
The University of Hong Kong
Pokfulam Road, Hong Kong, P. R. China
E-mail: yangdan@hku.hk
[b] Dr. N. Hananya, Dr. O. Green, and Prof. Dr. D. Shabat
School of Chemistry, Faculty of Exact Sciences
Tel Aviv University
Tel Aviv 69978 (Israel)
E-mail: chdoron@post.tau.ac.il
[c] Dr. H.-S. Chen, Prof. Dr. J.-G. Shen
School of Chinese Medicine
The University of Hong Kong
Pokfulam Road, Hong Kong, P. R. China
[+] These two authors made equal contribution to this paper.

Table of Contents

1. General methods

All reactions requiring anhydrous conditions were performed under an argon atmosphere. All reactions were carried out at room temperature unless stated otherwise. Chemicals and solvents were either A.R. grade or purified by standard techniques. Thin layer chromatography (TLC): silica gel plates Merck 60 F254: compounds were visualized by irradiation with UV light. Column chromatography (FC): silica gel Merck 60 (particle size 0.040-0.063 mm), eluent given in parentheses. Reverse-phase high pressure liquid chromatography (RP-HPLC): C18 5u, 250x4.6mm, eluent given in parentheses. Preparative RP-HPLC: C18 5u, 250x21mm, eluent given in parentheses. ^{1}H-NMR spectra were recorded using Bruker Avance operated at 300 MHz or 400MHz. ^{13}C-NMR spectra were recorded using Bruker Avance operated at 75 MHz or 100 MHz. Chemical shifts were reported in ppm on the δ scale relative to a residual solvent ($CDCl_3$: δ = 7.26 for ^{1}H-NMR and for 77.16 ^{13}C-NMR). Mass spectra were measured on Waters Xevo TQD. Chemiluminescence was recorded on Molecular Devices Spectramax i3x or Hitachi F-7000 spectrophotometer using a chemiluminescent mode. Fluorescence quantum yield was determined using Hamamatsu Quantaurus-QY. Chemiluminescent imaging was carried out on Perkin Elmer IVIS Spectrum In Vivo Imaging System. Peroxynitrite was synthesized as reported.[1] Peroxynitrite solution was split into small aliquots and frozen at temperature below –18 °C. All reagents, including salts and solvents, were purchased from Sigma-Aldrich. Light irradiation for photochemical reactions: LED PAR38 lamp (19W, 3000K).

Abbreviations. ACN: Acetonitrile; **DCM**: Dichloromethane; **DMF**: N,N'-Dimethylformamide; **EtOAc**: Ethyl acetate; **Hex**: Hexane; **TFA**: Trifluoroacetic acid; **THF**: Tetrahydrofuran.

2. Synthesis and characterization of H_2O_2-CL-510

General synthetic scheme

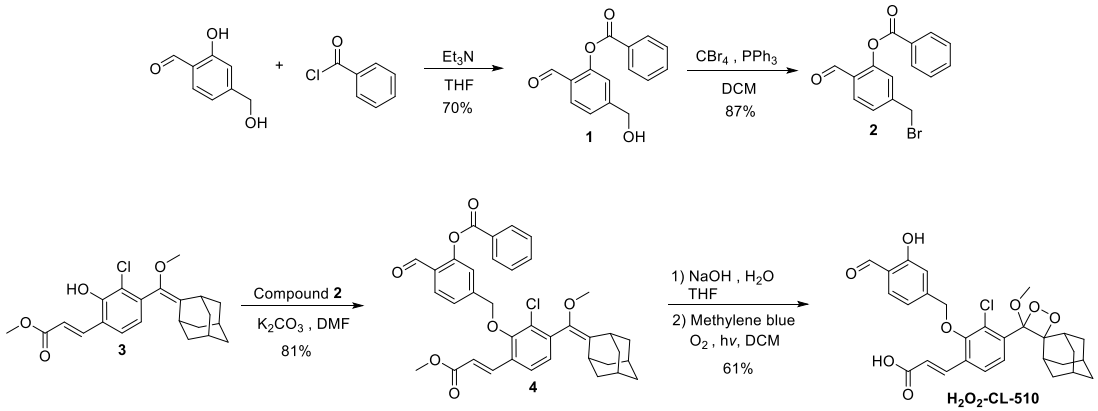

Procedures

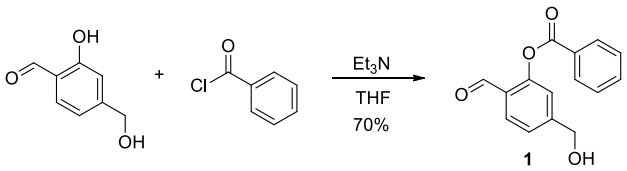

Compound 1

Triethylamine (150 µL, 1.1 mmol) and 4-hydroxymethylsalicylaldehyde (152 mg, 1 mmol) were dissolved in 5 mL THF and cooled to 0°C. Then, benzoyl chloride (115 µL, 1 mmol) was added and the solution stirred for 30 minutes and monitored by TLC (Hex:EtOAc 70:30). After full consumption of starting material, the reaction mixture was diluted with EtOAc (100 ml) and washed with brine (50 mL). The organic layer was separated, dried over Na_2SO_4 and evaporated under reduced pressure. The crude product was purified by column chromatography on silica gel (Hex:EtOAc 70:30). Compound **1** was obtained as a white solid (180 mg, 70% yield). ^{1}H-NMR (300 MHz, $CDCl_3$) δ 10.23 (s, 1H), 8.32 (d, *J* = 7.2 Hz, 2H), 7.97 (d, *J* = 7.8 Hz, 1H), 7.79 (t, *J* = 7.4 Hz, 1H), 7.64 (t, *J* = 7.8 Hz, 2H), 7.48 – 7.40 (m, 2H), 4.81 (s, 2H), 3.57 (br, 1H); ^{13}C-NMR (75 MHz, $CDCl_3$) δ 188.39, 165.13, 152.22, 149.93, 134.09, 130.41, 130.23, 128.72, 128.44, 126.94, 124.10, 121.04, 63.60; LRMS (EI, 20 ev): *m/z* (%) 256 (M^+; 1), 105 (100); HRMS (EI): calcd for $C_{15}H_{12}O_4$ (M^+): 256.0736, found: 256.0731.

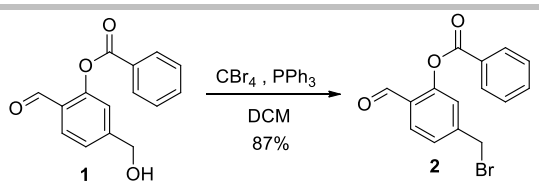

Compound 2

To a solution of compound **1** (150 mg, 0.58 mmol) and CBr_4 (580 mg, 1.75 mmol) in DCM (100 mL) was added triphenylphosphine (460 mg, 1.75 mmol) at 0 °C. The mixture was stirred at room temperature for 60 minutes and monitored by TLC (Hex:EtOAc 80:20). After full consumption of starting material, the reaction mixture was diluted with EtOAc (100 mL) and washed with brine (50 ml). The organic layer was separated, dried over Na_2SO_4 and evaporated under reduced pressure. The crude product was purified by column chromatography on silica gel (Hex:EtOAc 80:20). Compound **2** was obtained as a white solid (160 mg, 87% yield). ^{1}H-NMR (300 MHz, $CDCl_3$) δ 10.18 (s, 1H), 8.22 (d, *J* = 7.3 Hz, 2H), 7.93 (d, *J* = 8.0 Hz, 1H), 7.69 (t, *J* = 7.4 Hz, 1H), 7.55 (t, *J* = 7.8 Hz, 2H), 7.44 (d, *J* = 8.1 Hz, 1H), 7.38 (s, 1H), 4.50 (s, 2H).; ^{13}C-NMR (75 MHz, $CDCl_3$) δ 187.81, 164.91, 152.44, 145.55, 134.34, 130.74, 130.47, 128.94, 128.54, 128.05, 127.12, 124.21, 31.38; LRMS (EI, 20 ev): *m/z* (%) 318.0 (M^+; 1), 320 (M^+; 1), 105 (100); HRMS (EI): calcd for $C_{15}H_{11}BrO_3$ (M^+): 317.9892, 319.9871, found: 317.9880, 319.9860.

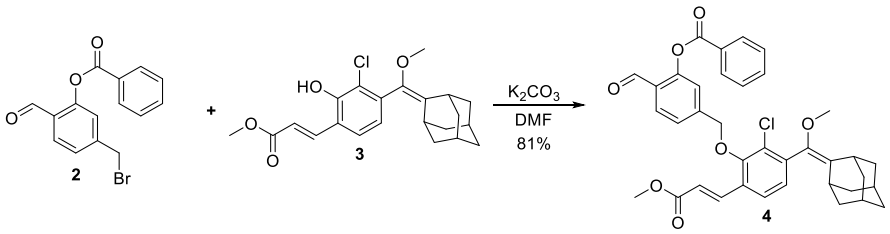

Compound 4

Phenol enol ether **3**[2] (120 mg, 0.31 mmol) and K_2CO_3 (86 mg, 0.6 mmol) were dissolved in DMF (2 mL). The solution was stirred for 5 minutes before compound **2** (100 mg, 0.31 mmol) was added. The reaction mixture was stirred at room tempreture and monitored by TLC (Hex:EtOAc 80:20). After completion, the reaction mixture was diluted with EtOAc (100 mL) and washed with 0.1M HCl (50 mL) and brine (50 mL). The organic layer was separated, dried over Na_2SO_4 and evaporated under reduced pressure. The crude product was purified by column chromatography on silica gel (Hex:EtOAc 85:15). Compound **4** was obtained as a white solid (157 mg, 81% yield). ^{1}H-NMR (300 MHz, $CDCl_3$) δ 10.21 (s, 1H), 8.24 (d, *J* = 7.1 Hz, 2H), 7.99 (d, *J* = 7.9 Hz, 1H), 7.92 (d, *J* = 16.2 Hz, 1H), 7.68 (t, *J* = 7.4 Hz, 1H), 7.60 – 7.52 (m, 3H), 7.51 (s, 1H), 7.47 (d, *J* = 8.1 Hz, 1H), 7.11 (d, *J* = 8.0 Hz, 1H), 6.48 (d, *J* = 16.2 Hz, 1H), 5.10 (d, *J* = 2.2 Hz, 2H), 3.76 (s, 3H), 3.33 (s, 3H), 3.27 (s, 1H), 2.08 (s, 1H), 1.97 – 1.70 (m, 12H); ^{13}C-NMR (75 MHz, $CDCl_3$) δ 188.16, 167.07, 165.03, 153.49, 152.58, 144.50, 139.40, 138.49, 138.43, 134.25, 132.94, 130.59, 130.52, 129.72, 129.60, 128.92, 128.77, 128.32, 128.14, 125.78, 125.37, 122.89, 120.63, 74.59, 57.48, 51.98, 39.34, 39.18, 38.78, 37.16, 33.10, 29.87, 28.46, 28.31; LRMS (ESI, +ve): m/z calc. for $C_{37}H_{35}ClO_7$: 626.2; found: 649.4 $[M+Na]^+$; HRMS (ESI, +ve): m/z calc. for $C_{37}H_{36}ClO_7$($[M+H]^+$): 627.2144; found: 627.2144.

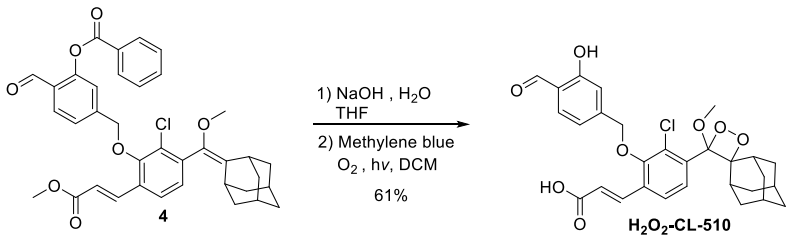

Compound H_2O_2-CL-510

Compound **4** (50 mg, 0.08 mmol) and NaOH (20 mg, 0.5 mmol) were dissolved in 5 mL solution of 4:1 THF:H_2O. Reaction mixture was stirred at 60 °C and monitored by RP-HPLC. Upon completion, the reaction mixture was diluted with EtOAc (50 ml) and washed with saturated solution of 0.1M HCl (25 mL) and brine (25 mL). The organic layer was separated, dried over Na_2SO_4 and evaporated under reduced pressure. The crude residue and a catalytic amount of methylene blue (~1 mg) were dissolved in 10 mL of DCM. Oxygen was bubbled through the solution while irradiating with yellow light. The reaction was monitored by RP-HPLC. Upon completion, the solvent was concentrated under reduced pressure and the product was purified by preparative RP-HPLC (gradient of ACN in water). Compound **H_2O_2-CL-510** was obtained as a white solid (26 mg, 61% yield). ^{1}H-NMR (400 MHz, $CDCl_3$) δ 11.06 (s, 1H), 9.91 (s, 1H), 8.38 (s, 1H), 8.07 – 7.89 (m, 2H), 7.65 – 7.59 (m, 2H), 7.17 (d, *J* = 7.9 Hz, 1H), 7.12 (s, 1H), 6.52 (d, *J* = 16.1 Hz, 1H), 4.95 (s, 2H), 3.23 (s, 3H), 3.03 (s, 1H), 2.30 (d, *J* = 12.0 Hz, 1H), 2.01 – 1.31 (m, 12H); ^{13}C-NMR (100 MHz, $CDCl_3$) δ 196.21, 171.32, 161.81, 154.18, 145.34, 140.08, 135.92, 134.10, 131.04, 129.36, 127.70, 125.57, 120.92, 120.43, 119.19, 116.84, 111.65, 96.39, 75.17, 49.74, 36.55, 33.89, 33.62, 32.67, 32.19, 31.56, 29.68, 26.14, 25.81; LRMS (ESI, −ve): m/z calc. for $C_{29}H_{29}ClO_8$: 540.2; found: 539.4 $[M–H]^-$; HRMS (ESI, +ve): m/z calc. for $C_{29}H_{29}ClNaO_8$($[M+Na]^+$): 563.1443; found: 563.1432.

3. Preparation of analyte solutions

ROO•: Alkylperoxyl radical was generated from 2,2'-azobis(2-amidinopropane) dihydrochloride (10 mM), which was added into the testing solutions directly.

$^1O_2$: Singlet oxygen was generated from 3,3'-(naphthalene-1,4-diyl)dipropionic acid (10 mM).

•NO: Nitric oxide was generated from SNP (sodium nitroferricyanide(III) dihydrate) (10 mM).

TBHP: *tert*-Butyl hydroperoxide solution (10 mM) was added into the testing solutions directly.

$O_2^{\bullet-}$: Superoxide was generated from xanthine/xanthine oxidase system. Xanthine oxidase (0.1 U/mL) was added before xanthine (30 mM). Catalase was added to remove the H_2O_2 produced in the system.

HOCl: NaOCl solution (10 mM) was added directly.

•OH: Hydroxyl radical was generated by Fenton reaction. To generate •OH, ferrous chloride was added in the presence of H_2O_2. The concentration of •OH was equal to the Fe(II) concentration (10 mM).

$ONOO^-$: Peroxynitrite solution was synthesized according to literature report.[1] The concentration of peroxynitrite was determined by measuring the absorption of the solution at 302 nm. The extinction coefficient of peroxynitrite solution in 0.1 M NaOH is 1,670 M^{-1} cm^{-1} at 302 nm.

H_2O_2: H_2O_2 solution (10 mM) was added directly.

4. Chemiluminescence emission spectra of H_2O_2-CL-510 with or without H_2O_2

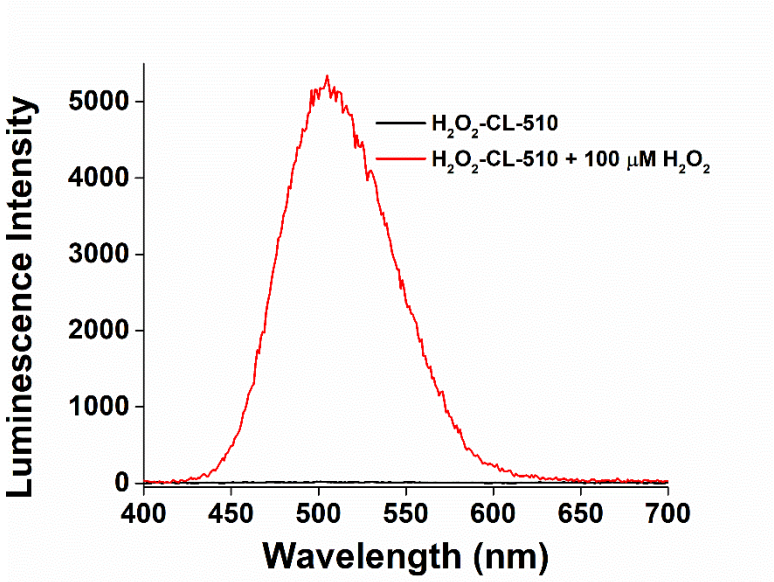

Figure S1. Chemiluminescence emission spectra of **H_2O_2-CL-510** (10 μM, supplemented with 100 μM CCl_3CN) with or without 100 μM H_2O_2. Measurements were conducted at 3 min after H_2O_2 addition in potassium phosphate buffer, pH 7.4, 37°C.

5. Reproducibility tests of chemiluminescence measurement and imaging

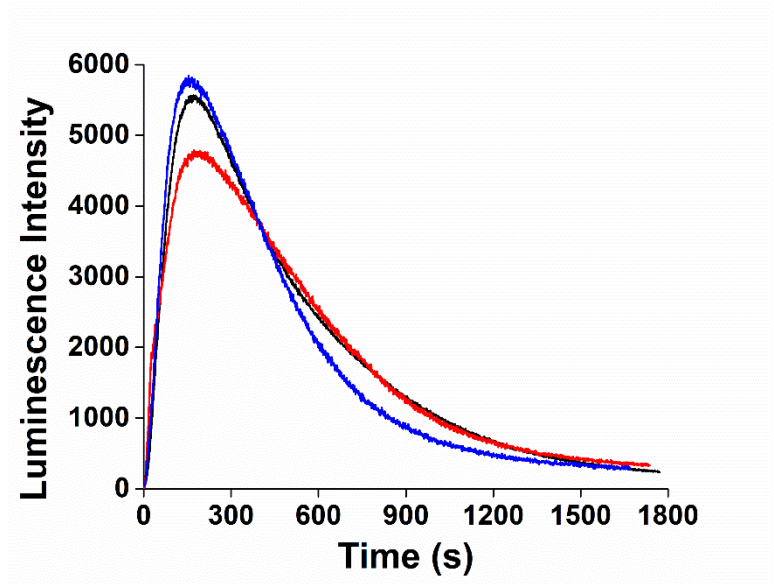

Figure S2. Time courses of **H_2O_2-CL-510** (10 μM) reacted with 100 μM H_2O_2 in triplicates: first trial in black, second trial in blue, and third trial in red. Measurements were conducted at potassium phosphate buffer, pH 7.4, 37°C.

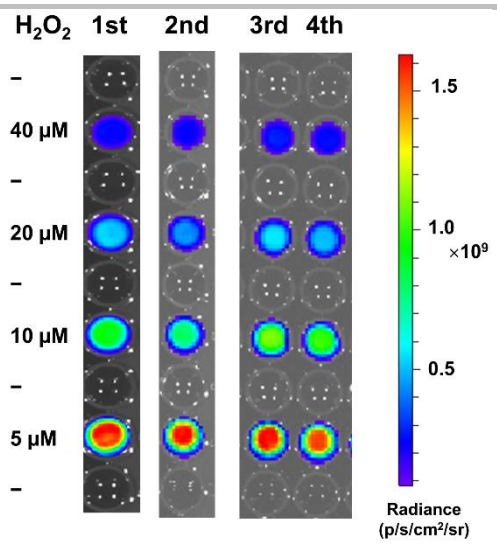

Figure S3. Luminescent images of **H_2O_2-CL-510** (10 μM) treated with increasing amounts of H_2O_2 (0–40 μM) in quadruplicates. The images were acquired at 2–3 min after H_2O_2 addition.

6. Cell culture, animal model and chemiluminescent imaging

Leukemia cells THP-1 were cultured in RPMI 1640 medium supplemented with 10% heat-inactivated fetal bovine serum (Gibco) and 1% penicillin/streptomycin, at 37 °C with 5% CO_2. One day before imaging, THP-1 cells were typically seeded at a density of 2×10^5 cells/mL in 96-well plates (Corning). For acute H_2O_2 induction, arsenic trioxide (0–32 μM) was added to RPMI 1640 medium and co-incubated with cells for 24 hours. Stock solutions (10 mM) of chemiluminescent probe, **H_2O_2-CL-510**, were prepared in anhydrous DMF. 200 U cell-permeable catalase-polyethylene glycol was added into intervention groups to remove cellular H_2O_2. Cells were spin down, and washed with PBS before the addition of chemiluminescent probe (10 μM final concentration) in 0.1 mL HBSS (Hank's balanced salt solution containing100 μM CCl_3CN) in each well. Cells were typically incubated with **H_2O_2-CL-510** for 1 min before chemiluminescent imaging.

Animal experimental protocols were conducted in accordance with the national and institutional guidelines on ethics and biosafety, which were approved and regulated by the Committee on the Use of Live Animals in Teaching and Research (CULATR), HKU. Cerebral ischemia-reperfusion was induced with a middle cerebral artery occlusion (MCAO) model similarly as previously described.[3] Briefly, rats were anesthetized with 4% isofluorane, and maintained at 2% isoflurane during surgery. Silicon-coated suture (Doccol, Redlands, CA, USA) was inserted from the external carotid artery to the internal carotid artery to occlude the middle cerebral artery. During the cerebral ischemia-reperfusion process, blood flow was monitored by using a Laser Doppler. At 2 h of cerebral ischemia, the intraluminal suture was withdrawn, and the common carotid artery was released to permit reperfusion for 1 h. For the sham control group, the surgical process was the same as the MCAO group without suture occlusion. Before imaging on IVIS Spectrum In Vivo Imaging System (PE-IVIS), 1 μL **H_2O_2-CL-510** (10 mM in DMF) and 4 μL CCl_3CN (10 mM in water) were injected into rat ventricle. Images were typically acquired after 6, 9, 12 min injection with an acquisition time of 2 min.

7. Cytotoxicity assay

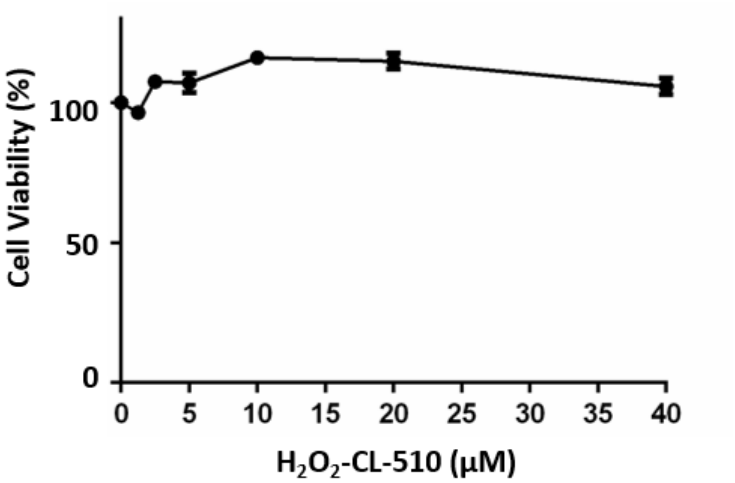

Figure S4. Cytotoxicity of **H_2O_2-CL-510** in RAW264.7 cells. RAW264.7 cells were incubated with increasing concentrations (1.25–40 μM) of **H_2O_2-CL-510** for 24 h. **H_2O_2-CL-510** (up to 40 μM) showed negligible or no cytotoxicity after 24 h incubation. Data represent mean ± s.e.m. with Cell-Titer Glo® assays performed in quadruplicates.

To assess potential toxicity of **H_2O_2-CL-510**, RAW264.7 cells were seeded at 2×10^5 cells/mL in 100 μL DMEM per well in a 96-well microplate (Corning). Cells were seeded one day in advance to allow their attachment on 96-well microplate. Stock solutions of **H_2O_2-CL-510** probes at various concentrations in DMF were added at testing concentrations (1.25–40 μM, final concentrations) into fresh medium. Seeded cells were incubated with **H_2O_2-CL-510**-containing medium (100 μL per well) for 24 h, then treated with 50 μL Cell-Titer Glo® reagent, followed by gentle shaking for 10 min at room temperature. Luminescence of cellular ATP could be used as indicator of cell viability, and luminescence of each well was measured on DTX 880 multimode plate reader. Cell viability was calculated according to the equation: Cell viability (%) = $100 \times A_{\text{with probe}} / A_{\text{control}}$, where A = luminescence intensity.

8. *In vivo* chemiluminescent imaging of rat brain during ischemia-reperfusion injury

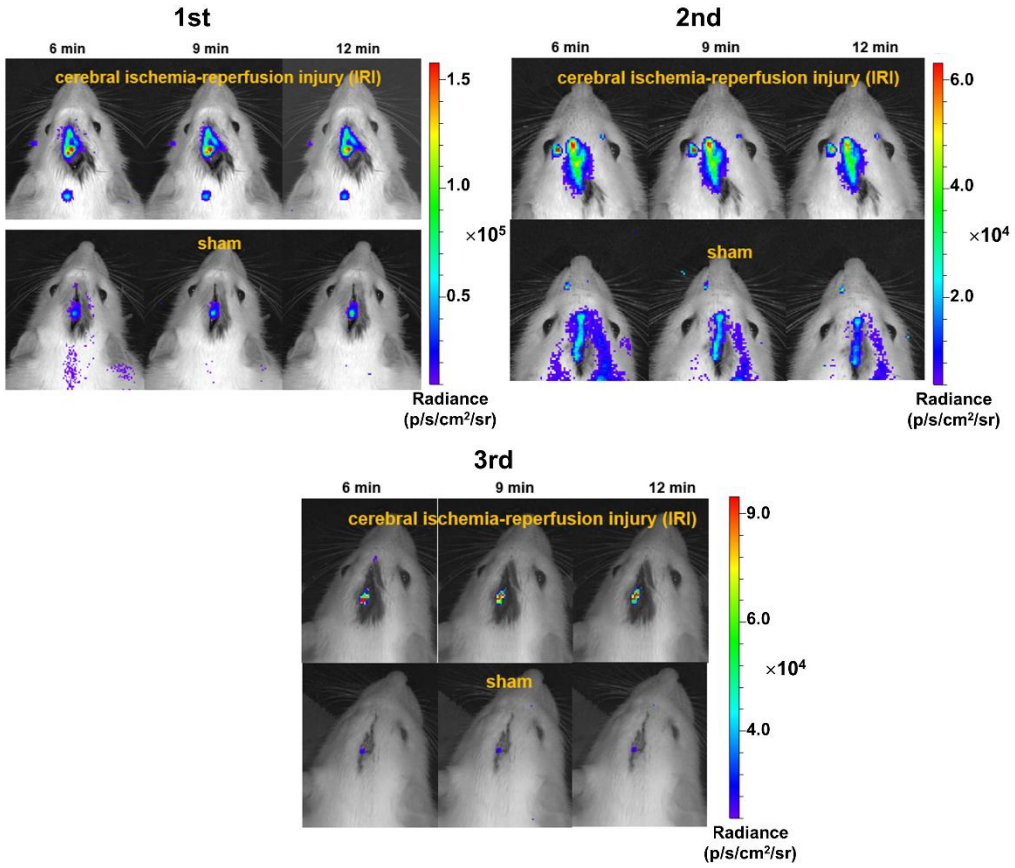

Figure S5. *In vivo* chemiluminescent imaging of **H_2O_2-CL-510** in response to H_2O_2 production in rat brain during ischemia-reperfusion injury. **H_2O_2-CL-510** (1 μL 10 mM in DMF mixed with 4 μL 10 mM CCl_3CN in water) was intraventricularly injected into rat brain before imaging. Independent experiments were carried out in triplicates.

9. H_2O_2 detection with fluorescent probe in brain tissue

Rats were subjected to MCAO ischemia-reperfusion as previously described, and sham operation was used as control. Rats were transcardially perfused with PBS, and brain samples was then collected for frozen section at a thickness of 20 μm. Brain samples were stained with a red H_2O_2 fluorescent probe, **HKPerox-4**,[4] (10 μM in HBSS supplemented with 100 μM CCl_3CN) for 30 min at room temperature, and fluorescence images were obtained by using a fluorescence microscope (Carl Zeiss) with Axio Vision digital imaging system.

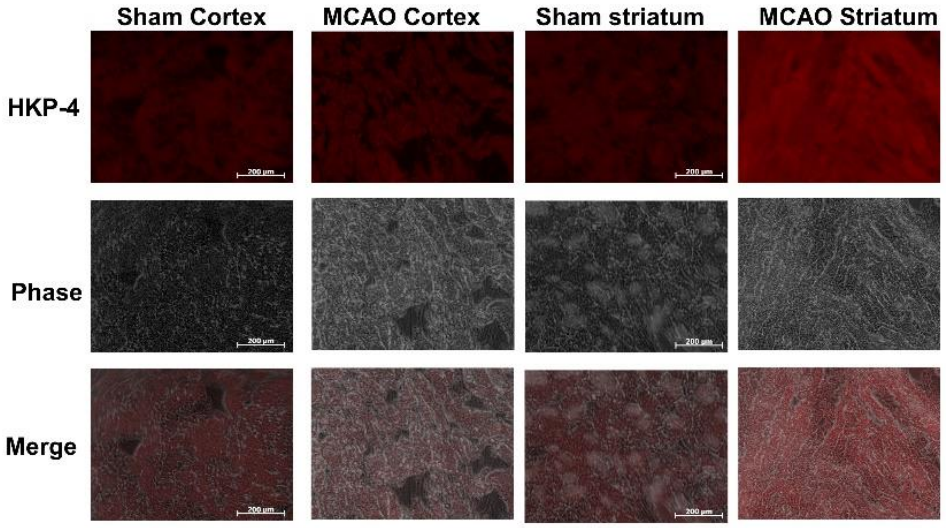

Figure S6. Representative fluorescent images of ischemia-reperfused brain tissue (cortex or striatum) stained with **HKPerox-4** (10 μM), scale bars represent 200 μm.

10. NMR spectra

^{1}H-NMR Spectra of **compound 1**

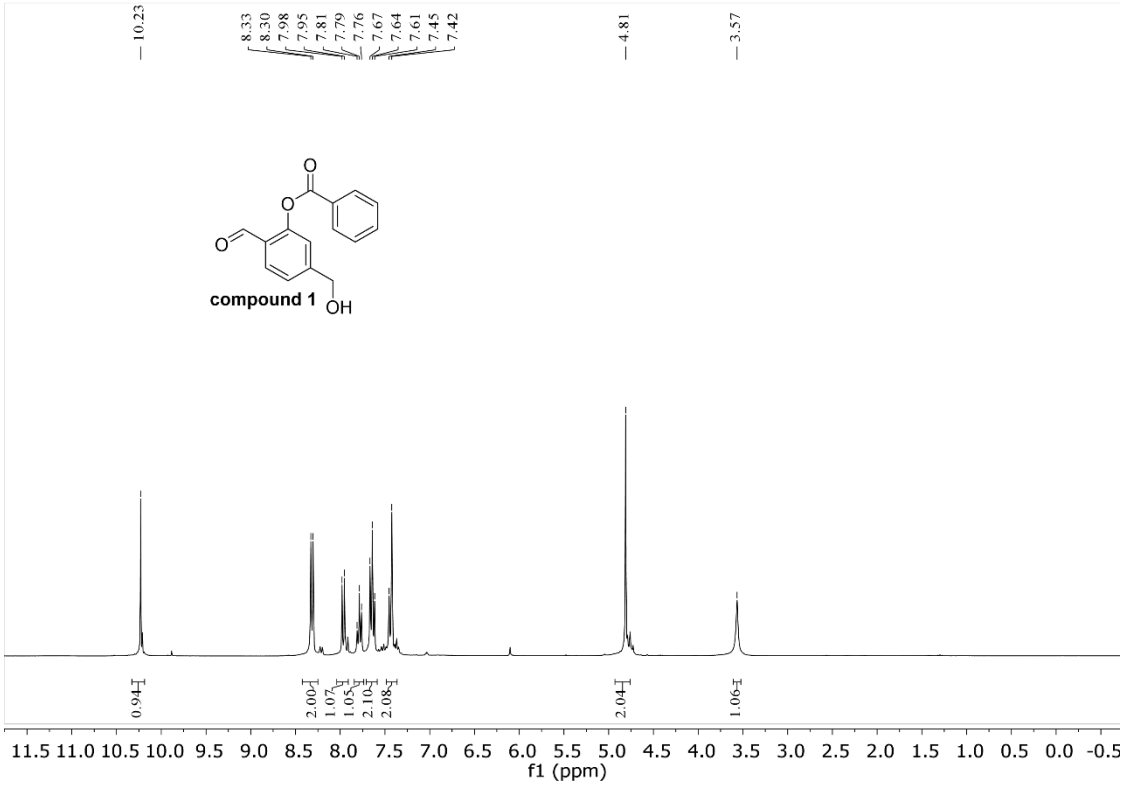

^{13}C-NMR Spectra of **compound 1**

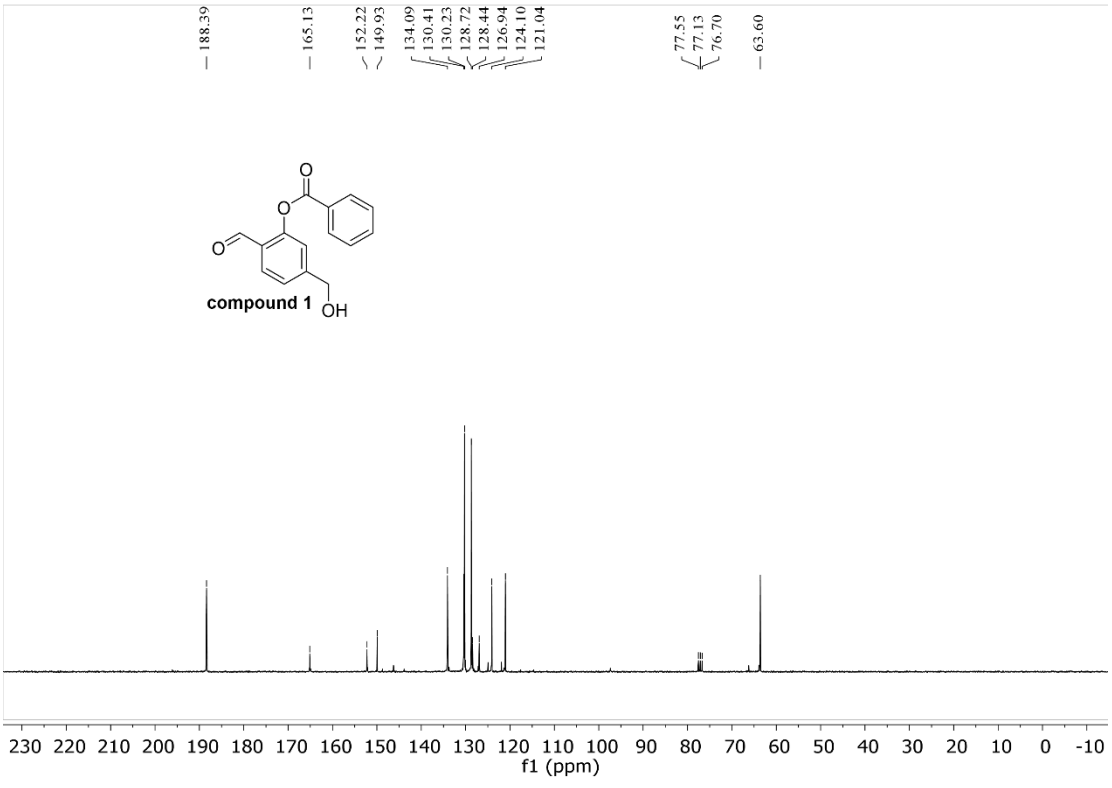

[1]H-NMR Spectra of **compound 2**

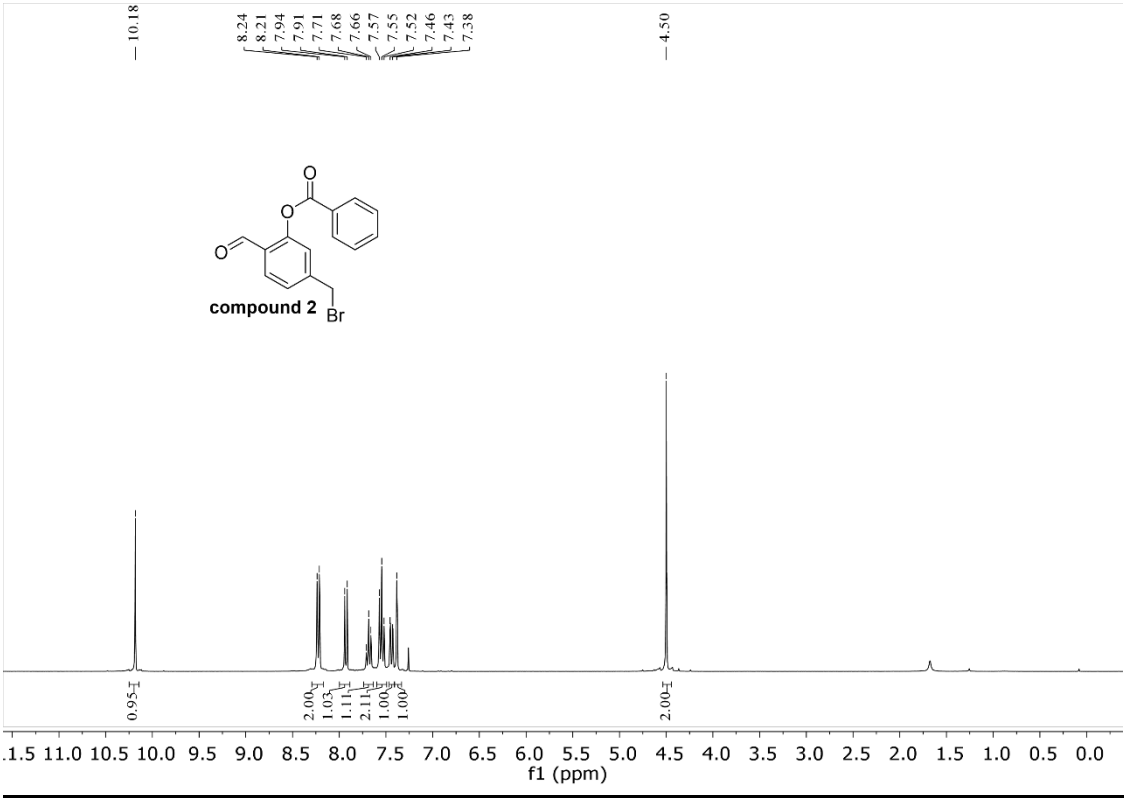

[13]C-NMR Spectra of **compound 2**

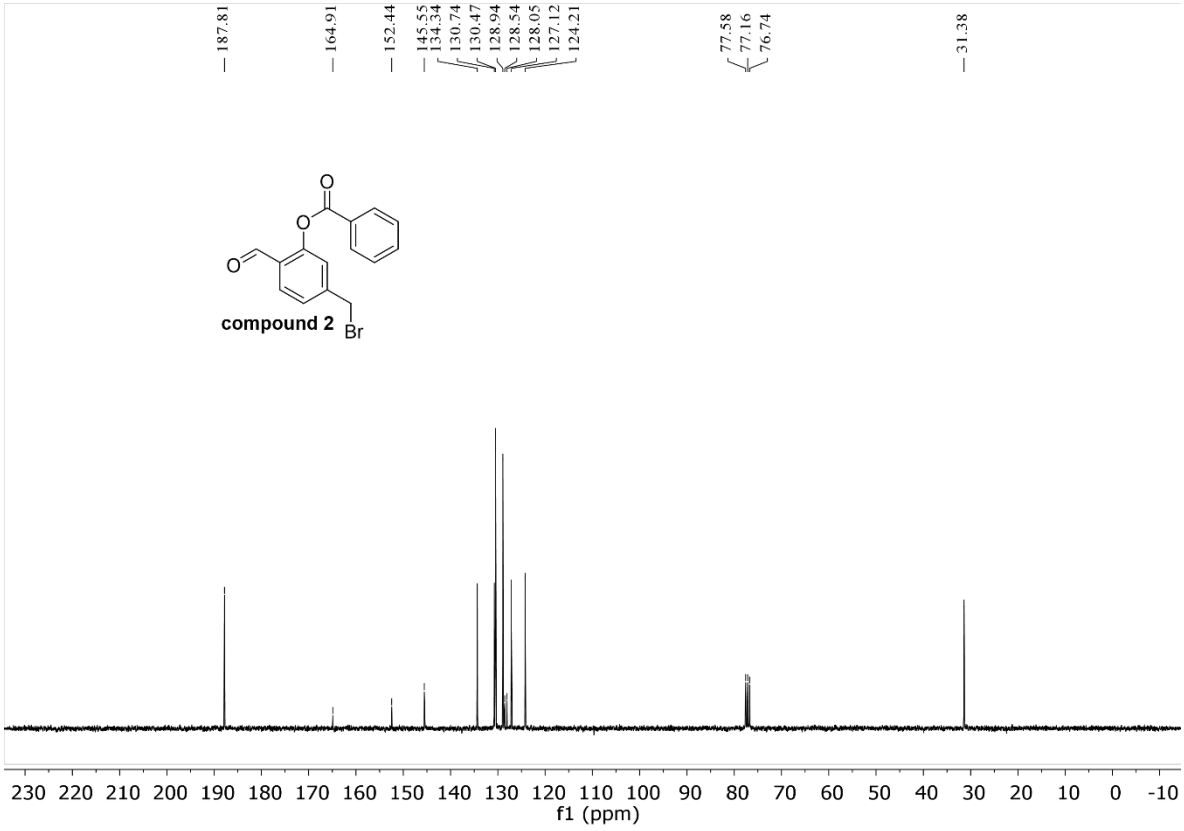

SUPPORTING INFORMATION

[1]H-NMR Spectra of **compound 4**

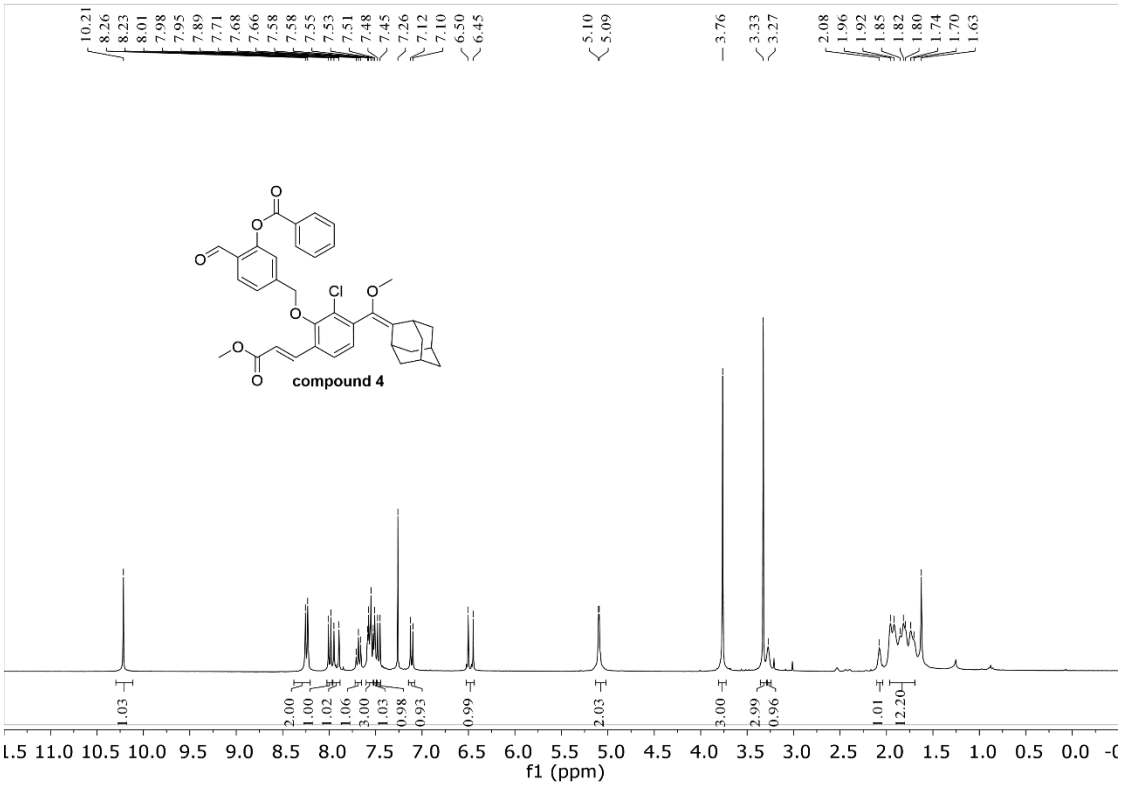

[13]C-NMR Spectra of **compound 4**

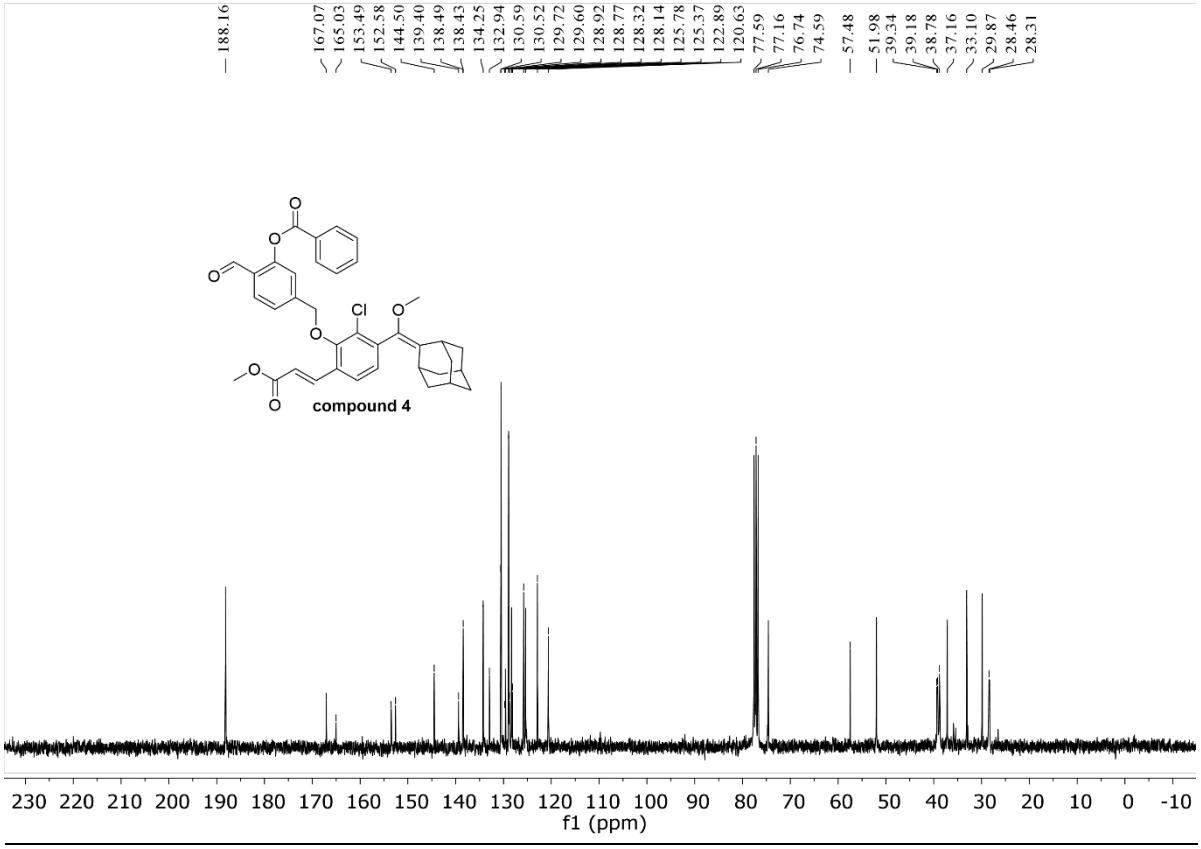

SUPPORTING INFORMATION

^{1}H-NMR Spectra of **H_2O_2-CL-510**

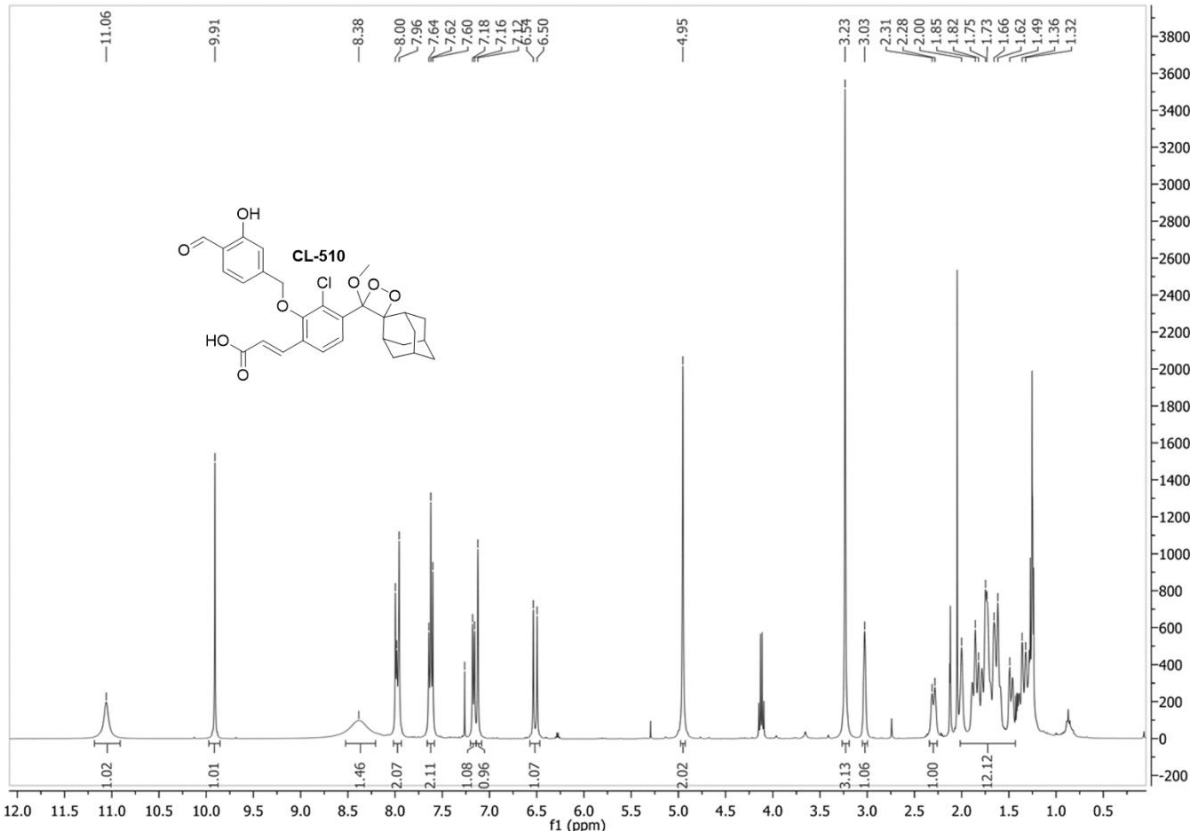

^{13}C-NMR Spectra of **H_2O_2-CL-510**

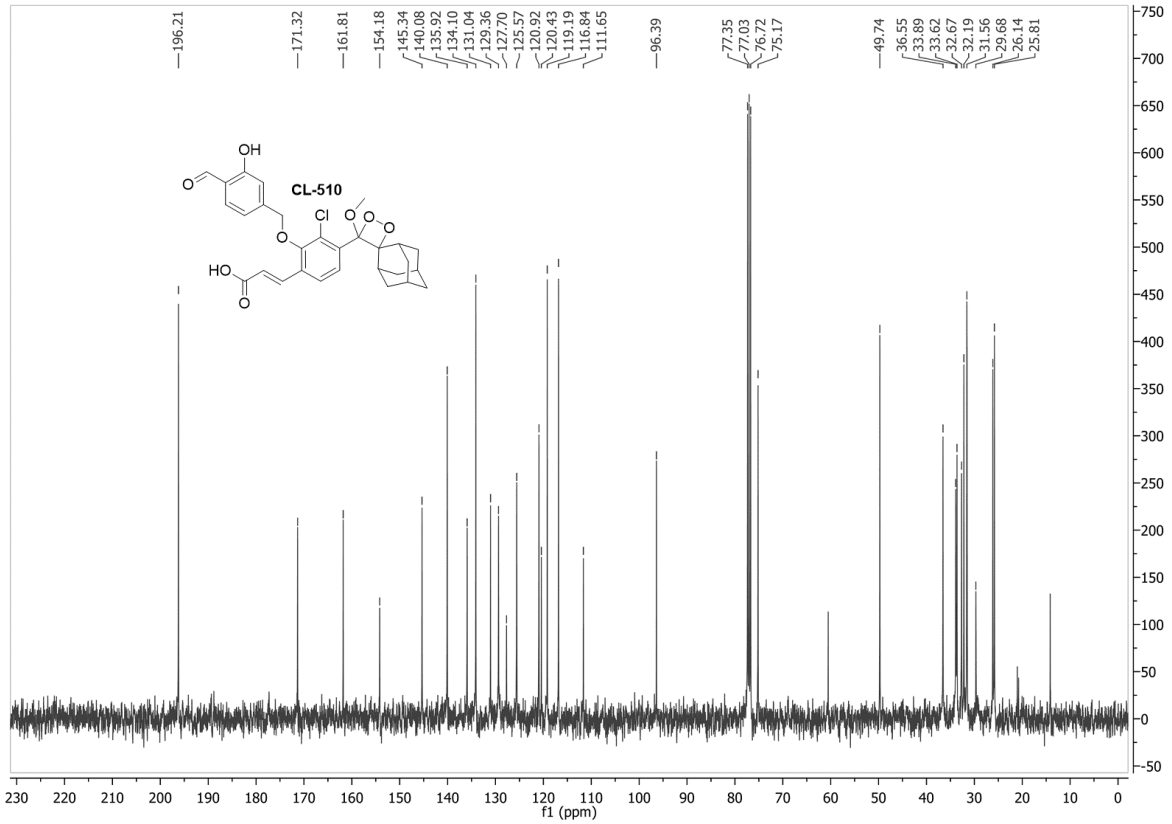

11. References

[1] J. W. Reed, H. H. Ho, W. L. Jolly, *J. Am. Chem. Soc.* **1974**, *96*, 1248-1249.
[2] O. Green, T. Eilon, N. Hananya, S. Gutkin, C. R. Bauer, D. Shabat, *ACS Cent. Sci.* **2017**, *3*, 349-358.
[3] H.-S. Chen, X.-M. Chen, J.-H. Feng, K.-J. Liu, S.-H. Qi, J.-G. Shen, *CNS Neurosci. Ther.* **2015**, *21*, 585-590.
[4] **HKPerox-4** is a red fluorescent H_2O_2 probe described as **YS-4-112** in following patent: D. Yang, S. Ye, J. J. Hu, *Compounds and methods for detection of hydrogen peroxide*, **2018**, PCT Appl. No.: WO2018133859.